Acta Cryst. (1951). **4**, 216

The Crystal Structure of $NaAlCl_4$

BY N. C. BAENZIGER*

Department of Research in Chemical Physics, Mellon Institute, Pittsburgh, Pennsylvania, U.S.A.

(*Received* 24 *July* 1950)

The crystal structure of $NaAlCl_4$ has been determined with data obtained from Weissenberg diagrams. The space group is $P2_12_12_1$, and the unit-cell dimensions are $a=10{\cdot}36$, $b=9{\cdot}92$, $c=6{\cdot}21$ A. With four molecules per unit cell, the calculated density is 2·00 g.cm.$^{-3}$. The co-ordinates of the atoms were found from electron-density projections on (100), (010) and (001). The structure consists of Na^+ and $AlCl_4^-$ ions. Interatomic distances from ion to ion are normal, but the Al–Cl (2·13 A.) and the Cl–Cl (3·48 A.) distances in the $AlCl_4^-$ tetrahedra are shorter than the normal distances.

Introduction

The system $NaCl$–$AlCl_3$ has been studied by several investigators (Kendall, Crittenden & Miller, 1923; Shvartsman, 1940: Chrétien & Lous, 1943) who found only one compound, $NaAlCl_4$, to exist in the system. An interesting use for the compound has been its application as a catalyst in the Friedel and Crafts reaction in organic chemistry (Norris & Klemka, 1940), its catalytic activity usually being explained on the assumption that it forms Na^+ and $AlCl_4^-$ ions. This communication describes the determination of the structure of $NaAlCl_4$ in the solid state and establishes the presence of these ions in the crystalline compound.

Preparation of crystal specimens

$NaAlCl_4$ was prepared by fusing equimolar amounts of NaCl and freshly sublimed $AlCl_3$ in a 'dry box'. (The 'dry box' was a gas-tight metal box with a large plastic window on the top providing visual access and rubber gloves sealed in the side providing manual access to the interior of the box. The box was thoroughly flushed with dry nitrogen and the atmosphere was dried further by trays of P_2O_5 for a period of a day prior to use.) A large number of crystals were selected from the melt during repeated fusions and solidifications. The best crystals were then mounted in thin-walled pyrex capillaries. All these manipulations were performed in the 'dry box'. The crystals mounted in this fashion kept for months, whereas those mounted and exposed in air absorbed moisture and disintegrated before the X-ray exposure was complete. Different crystals were mounted for rotation about each of the three crystallographic axes.

Diffraction data

Weissenberg diagrams prepared by rotation of the crystal about the three crystallographic axes revealed that the structure could be based on a primitive orthorhombic lattice with unit-cell dimensions

$$a=10{\cdot}36, \quad b=9{\cdot}92, \quad c=6{\cdot}21 \text{ A.}$$

The density of $NaAlCl_4$ calculated on the basis of four molecules per unit cell is 2·00 g.cm.$^{-3}$. The density found by Chrétien & Lous was 2·013 g.cm.$^{-3}$. The only systematic absences of reflections which were observed are $(h00)$ for h odd, $(0k0)$ for k odd, and $(00l)$ for l odd. From these absences the most probable space group is $P2_12_12_1$.

All X-ray diffraction data were obtained using Cu $K\alpha$ radiation with $\lambda=1{\cdot}5418$ A. The intensities of the diffraction maxima were estimated visually by comparison with standard films. In order to obtain standard comparison spots of the same shape as the spots whose intensities were to be determined, the standard films were prepared by taking a timed series of 6° Weissenberg exposures of a prominent reflection of the same crystal which was used to make the complete Weissenberg intensity films. Eighteen of these 6° Weissenberg exposures with a factor of approximately 1·2 between exposures were recorded side by side on the same film. Three films were used in the multiple-film technique for the standard comparison films and four multiple films were used for the Weissenberg intensity films to cover a larger range of darkening. A factor of 28 % (obtained from the standard comparison films) for the transmission of the double-coated Eastman X-ray film for Cu $K\alpha$ radiation was used in all the intensity comparisons between multiple films.

The observed F values, F_o's, were found from the intensities, I, according to the relation, $F_o \sim \sqrt{(I/LAP)}$, where L is the Lorentz factor, P is the polarization factor, and A is the absorption factor.

The crystals which could be successfully mounted were not quite small enough for the absorption factor to be neglected entirely. Since the crystals were small, however, an approximation to the true absorption factor was made in the following way. The apparent radius, R, that the crystal would have if it had a circular rather than rectangular cross-section was calculated. The absorption corrections for a cylindrical powder rod of radius R tabulated in the *Internationale Tabellen zur Bestimmung von Kristallstrukturen* were then used as the approximate absorption correction. This absorption

* Present address: Department of Chemistry and Chemical Engineering, State University of Iowa, Iowa City, Iowa, U.S.A.

approximation and the neglect of absorption by the pyrex capillary undoubtedly contribute to the occasional discrepancies between calculated and observed F values.

Structural investigation

The space group $P2_12_12_1$ has only the general position of multiplicity four:

4 (*a*) x, y, z; $\frac{1}{2}-x, \bar{y}, \frac{1}{2}+z$; $\frac{1}{2}+x, \frac{1}{2}-y, \bar{z}$; $\bar{x}, \frac{1}{2}+y, \frac{1}{2}-z$.

Bragg–Lipson plots (Bragg & Lipson, 1936) of the strong reflections (060), (590) and (530) limit most of the scattering material to small regions of x and y co-ordinates. With the assumption that the chlorine atoms would be located tetrahedrally around the aluminum atoms, the arrangement of the chlorine atoms on these allowed regions was restricted by spatial factors. For example, the small c dimension of the unit cell prohibited placing chlorine atoms directly above one another along the c axis. Therefore, the $AlCl_4^-$ tetrahedron could not be oriented so that one edge would be nearly parallel to the c axis. Likewise, the tetrahedra were excluded from the region of the twofold screw axes along c. In addition to these spatial factors the weakness of reflections of the type ($hk0$) when $h+k=2n+1$ indicated that the projection of scattering material on (001) was pseudo face-centered.

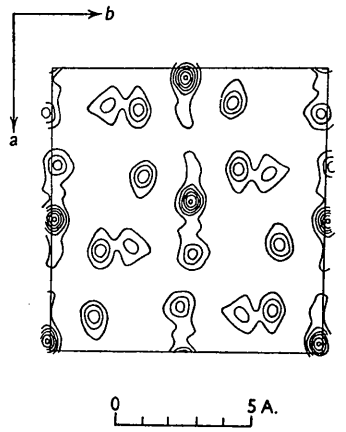

Fig. 1. Electron-density map, $\rho(x, y)$.

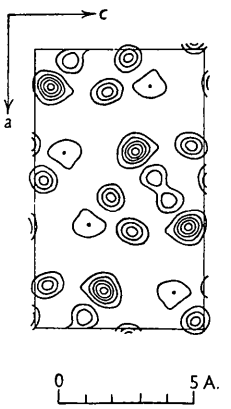

Fig. 2. Electron-density map, $\rho(x, z)$.

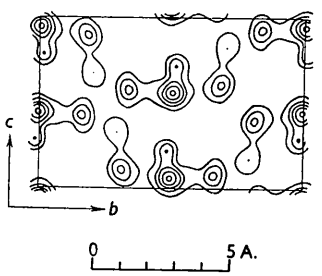

Fig. 3. Electron-density map, $\rho(y, z)$.

Several likely arrangements for the chlorine atoms were rapidly explored using these criteria. Numerical Bragg–Lipson charts for the strong reflections (590), (530), (1,10,0), (1,12,0), (490) and the absent or very weak reflections (320), (330), (340), (270), (930) as well as the ($h00$) and ($0k0$) reflections aided the trial-and-error process. An arrangement was soon found which gave reasonable agreement between calculated and observed F values. Using the signs of the F_c (calculated) values based on this structure a preliminary Fourier projection was made using about one-half of the observed F_o data. Subsequent projections, using more and finally all the observed $F_o(hk0)$ data (Fig. 1), changed the parameters only slightly but served to give more circular contours. (Points on all electron-density maps were evaluated at intervals of 1/60th of the unit-cell dimensions.)

The initial attempt to determine the z parameters was made using the ($h0l$) data. Approximate z parameters were readily determined using the ($00l$) data, the very strong (303) reflection, and known interatomic distances. A Fourier projection along the b axis on to (010), using nearly all the observed ($h0l$) data, gave atomic co-ordinates from which all the signs were determined for the second and final projection (Fig. 2).

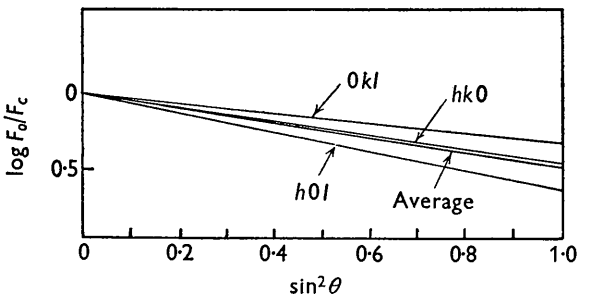

Fig. 4. Plots of $\log F_o/F_c$ versus $\sin^2\theta$.

Unfortunately, the two electron-density maps, $\rho(x, y)$ and $\rho(x, z)$, contained several superpositions of atoms so that not all the individual atomic co-ordinates could be determined. The electron-density map, $\rho(x, y)$, did not permit the x and y co-ordinates of the Cl_I and the Al atoms to be determined. The electron-density map, $\rho(x, z)$, permitted the determinations of the x and z co-ordinates of these atoms, but the peaks due to Cl_{II} and Cl_{IV} overlapped so that their x and z co-ordinates could not be determined from this plot.

In order to resolve these atomic positions, the ($0kl$) data were used to prepare $\rho(y, z)$ (Fig. 3). This electron-density plot enabled the z co-ordinates of Cl_{II} and Cl_{IV} to be determined as well as the y co-ordinate of the aluminum atom. The only undetermined atomic parameter remaining was the y parameter of Cl_I. The value of this parameter was chosen on the basis of the asymmetry of the superimposed peaks in the two projections.

Using the average parameters determined from the three electron-density maps, the F_c values were evaluated for all reflections. The values of $\log F_o/F_c$ plotted versus $\sin^2\theta$ gave slightly different slopes for the three sets of F values (Fig. 4). An average value for the temperature factor ($B=2{\cdot}67\times10^{-16}$) was then

chosen whose deviation from the individual temperature factors was within the error of intensity measurement. This average temperature factor was then included in the new calculated F_c values.

Fourier projections made using the temperature-corrected F_c values (Booth, 1946) gave peaks of electron density which were displaced from the positions obtained from the F_o data. The displacements Δx, Δy, Δz, are listed in Table 1 and may be considered indicative of the relative error in the atomic co-ordinates. F_c' values were then calculated on the basis of the co-ordinates obtained by applying the $\Delta x, \Delta y, \Delta z$, values with reversed sign as corrections to the original co-ordinates. The values of $R_1 = \Sigma \mid\mid F_o \mid - \mid F_c' \mid\mid / \Sigma \mid F_o \mid$ for the ($hk0$), ($h0l$), ($0kl$), and the (hkl) data (includes ($hk1$), ($hk2$), ($hk3$), and ($hk4$) data as well as ($hk0$), ($h0l$), and ($0kl$)) are given in Table 2. The values of the atomic parameters used in the structure-factor calculations are given in Table 3.

Table 1. *Displacement of electron-density peaks due to finite summation errors (in Ångström units)*

Atom	$\mid \Delta x \mid$	$\mid \Delta y \mid$	$\mid \Delta z \mid$
Cl_I	0·02	0·00	0·00
Cl_{II}	0·01	0·02	0·01
Cl_{III}	0·01	0·00	0·02
Cl_{IV}	0·02	0·02	0·01
Al	0·03	0·03	0·04
Na	0·01	0·00	0·04

Table 2. *Values of* $R_1 = \Sigma \mid\mid F_o \mid - \mid F_c' \mid\mid / \Sigma \mid F_o \mid$

($hk0$)	0·20
($0kl$)	0·26
($h0l$)	0·19
(hkl)	0·24

Table 3. *Atomic co-ordinates in* $NaAlCl_4$

Atom	x	y	z
Cl_I	0·031	0·490	0·552
Cl_{II}	0·148	0·316	0·105
Cl_{III}	0·348	0·024	0·923
Cl_{IV}	0·379	0·336	0·577
Al	0·039	0·485	0·204
Na	0·128	0·207	0·677

Discussion of the structure

The four $AlCl_4^-$ tetrahedra in the unit cell are arranged so that each has a face nearly parallel to the (001) plane. Each tetrahedron has one apex located so that chlorine atoms are approximately at the corners and centers of the faces of the unit cell. All the tetrahedra point downward along the c axis in the (010) plane and upward in the (020) plane. The centers of the tetrahedra thus lie nearly on the screw axes parallel to the b axis. A projection of the tetrahedra on (001) is shown in Fig. 5.

The chlorine atoms lie approximately in two layers perpendicular to the c axis. Fig. 6 shows the plan (projection on (001)) and Fig. 7 shows the elevation (projection on (100)) of these chlorine layers.

The chlorine–chlorine distances between adjacent tetrahedra range from 3·80 to 3·87 A. or slightly more than the sum of the ionic radii of chlorine atoms. The chlorine–chlorine distances within the nearly regular $AlCl_4^-$ tetrahedron are shorter than the ionic distance,

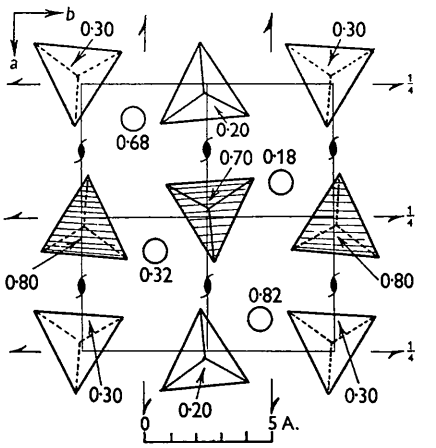

Fig. 5. Projection of $AlCl_4^-$ tetrahedra on (001).

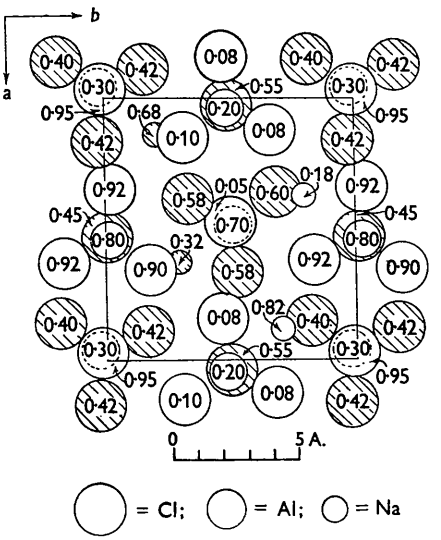

Fig. 6. Plan of chlorine layers—projection on (001).

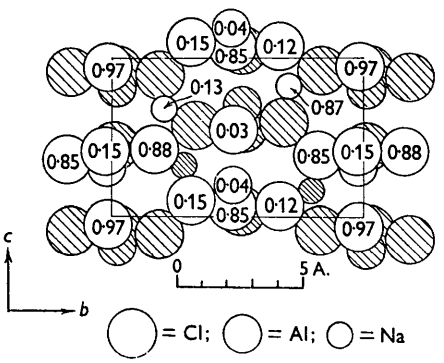

Fig. 7. Elevation of chlorine layers—projection on (100).

being on the average 3·48 A. The aluminum–chlorine distance, 2·13 A., is shorter than the sum of the tetrahedral covalent radii, 2·25 A. (Pauling, 1940, p. 179).

The shortening of the metal–halogen bond has been previously observed in the results of electron-diffraction studies of metal halide molecules in the vapor state. It has been pointed out by several observers (Schomaker & Stevenson, 1941; Burawoy, 1943; Warhurst, 1949) that a decrease in bond distance is to be expected as the bond acquires more ionic character. Another explanation (Pauling, 1940, p. 228) attributes the shortening to partial double-bond character of the bond. Either explanation is applicable to $AlCl_4$.

Table 4. *Interatomic distances (in Ångström units)*

Distances in the $AlCl_4^-$ tetrahedron

Cl_I –Cl_{II}	3·48	Al–Cl_I	2·16
Cl_I –Cl_{III}	3·51	Al–Cl_{II}	2·11
Cl_I –Cl_{IV}	3·54	Al–Cl_{III}	2·13
Cl_{II} –Cl_{III}	3·49	Al–Cl_{IV}	2·12
Cl_{II} –Cl_{IV}	3·46		
Cl_{III}–Cl_{IV}	3·39		

Other distances

Na–Cl_I	3·08	Cl_I–Cl_{II}	3·85	Cl_{II}–Cl_I	3·85
Cl_I	3·20	Cl_{II}	3·86	Cl_I	3·86
Cl_{II}	2·88	Cl_{II}	4·03	Cl_I	4·03
Cl_{II}	3·72	Cl_{III}	3·77	Cl_{III}	3·74
Cl_{III}	2·79	Cl_{III}	3·95	Cl_{III}	3·91
Cl_{III}	3·29	Cl_{IV}	3·69	Cl_{IV}	3·74
Cl_{IV}	2·96	Cl_{IV}	3·81	Cl_{IV}	3·79
Cl_{IV}	3·06	Cl_{IV}	3·92	Cl_{IV}	4·06
Cl_{III}–Cl_I	3·74	Cl_{IV}–Cl_I	3·69		
Cl_I	3·77	Cl_I	3·81		
Cl_I	3·95	Cl_I	3·92		
Cl_{II}	3·91	Cl_{II}	3·74		
Cl_{III}	3·74	Cl_{II}	3·79		
Cl_{III}	3·74	Cl_{II}	4·06		
Cl_{IV}	3·78	Cl_{III}	3·78		

The sodium ions are located in the empty spaces between the tetrahedra. All the sodium–chlorine distances are larger than the sum of ionic radii, 2·76 A. The sodium atom has seven chlorine neighbors from 2·79 to 3·29 A. distant with one chlorine atom much farther away at 3·72 A. Interatomic distances are listed in Table 4.

The author wishes to thank Dr H. P. Klug for suggesting and supporting this investigation and for helpful discussions in the preparation of this manuscript.

References

Booth, A. D. (1946). *Proc. Roy. Soc.* A, **188**, 77.

Bragg, W. L. & Lipson, H. (1936). *Z. Krystallogr.* **95**, 323.

Burawoy, A. (1943). *Trans. Faraday Soc.* **39**, 79.

Chrétien, A. & Lous, E. (1943). *C.R. Acad. Sci., Paris,* **217**, 451.

Kendall, J., Crittenden, E. D. & Miller, H. K. (1923). *J. Amer. Chem. Soc.* **45**, 963.

Norris, J. F. & Klemka, A. J. (1940). *J. Amer. Chem. Soc.* **62**, 1432.

Pauling, L. (1940). *The Nature of the Chemical Bond.* Ithaca: Cornell University Press.

Schomaker, V. & Stevenson, D. P. (1941). *J. Amer. Chem. Soc.* **63**, 37.

Shvartsman, U. I. (1940). *Zapiski Inst. Khim. Akad. Nauk. S.S.S.R.* **7**, No. 1, 3. Abstracted in *Chem. Abstr.* **35**, 2402².

Warhurst, E. (1949). *Trans. Faraday Soc.* **45**, 461.

Acta Cryst. (1951). **4**, 219

Rotatory Power and Other Optical Properties of Certain Liquid Crystals

By Hl. de Vries

Physical Laboratory of the University at Groningen, Netherlands

(*Received* 7 *July* 1950)

A group of liquid crystals, mainly derivates of cholesterol, shows remarkable optical properties, including strong rotatory power and selective reflexion of circularly polarized light in a narrow region of wave-lengths. In this paper it is shown how these properties can be explained by the assumption that the molecules are arranged in a special way, so that the electrical axes rotate screw-like. It is inessential whether this occurs in small steps or continuously. When the axes make one revolution over a thickness p, then light in a region around $\lambda = pn$ will be reflected (n = refractive index). The second important parameter is the value of the double refraction $\alpha = (n_2 - n_1)/n$. From p and α all optical properties can be calculated. No accurate data for testing the theory are available but qualitatively the agreement is complete.

1. Description of the phenomena

From a monograph by Friedel (1922), we may summarize the phenomena occurring for a group of liquid crystals, mainly cholesterol derivates, as follows:

(1) Strong rotatory power (see Fig. 1). It amounts to more than ten and even to hundreds of revolutions per mm., whereas quartz gives only 24°/mm.

(2) Whereas in normal substances wave-length regions of opposite sign of the rotatory power are separated by a region of *absorption*, the liquid crystals have a region of *reflexion* of circularly polarized light. One circularly polarized component of the incident beam is completely unaffected; for the substance characterized by Fig. 1 (type 'dextro') it is only the